Precision measurement of the $^{25}Mg^{+}$ ground-state hyperfine constant

Z. T. Xu, K. Deng,* H. Che, W. H. Yuan, J. Zhang, and Z. H. Lu†

MOE Key Laboratory of Fundamental Physical Quantities Measurement, Hubei Key Laboratory of Gravitation and Quantum Physics, School of Physics, Huazhong University of Science and Technology, Wuhan 430074, People's Republic of China

(Received 28 August 2017; published 21 November 2017)

We report an experimental determination of the ground-state hyperfine constant A of the $^{25}Mg^{+}$ ions by measuring the $|S_{1/2},F=2,m=0\rangle$ to $|S_{1/2},F=3,m=0\rangle$ transition (0-0 transition) frequency of the two ground-state hyperfine energy levels. The frequency is measured by rf resonant method in a Paul trap under a magnetic field of about 0.1 mT. The result is $A=-596.254\,248\,7(42)$ MHz. Different frequency shifts and uncertainties are evaluated. The main effect is quadratic Zeeman shift. Since the Paul trap is driven by rf on the electrodes, ac magnetic field can be induced by the rf at the site of the ion. The ac magnetic field causes quadratic Zeeman shift for ion frequency standards and also reduces the coherence time when the ion acts as a quantum bit. Precision measurement of this ac magnetic field can help evaluating the related uncertainty when a single-ion optical clock is established on the trap.

DOI: 10.1103/PhysRevA.96.052507

I. INTRODUCTION

Precision measurement of the ground-state hyperfine constants of the neutral alkali-metal atoms has led to great developments in microwave atomic frequency standards, such as Cs fountain clocks [1] and Rb fountain clocks [2]. Similar measurements have been done on singly ionized alkaline-earth atoms or singly ionized alkaline-earth-like atoms, such as Be^{+} [3], Mg^{+} [4], Ba^{+} [5,6], Cd^{+} [7], Hg^{+} [8], and Yb^{+} [9], with the primary goal of developing better microwave frequency standards. In addition, since hyperfine interactions are sensitive to electron correlations, precision measurements of the hyperfine constants provide important tests for atomic structure theory.

The ground-state magnetic-dipole hyperfine constant (A value) of $^{25}Mg^{+}$ ions has been theoretically investigated by several groups [10–14]. Precision measurement of the A value for free $^{25}Mg^{+}$ ions was reported in a Penning trap under a magnetic field of 1.24 T [4]. The hyperfine constant was deduced by measuring the frequencies of different transitions between different Zeeman sublevels. The relative uncertainty was about 9×10^{-8}. Since those works there has been no further report on a higher-precision measurement. For comparison, hyperfine constants measurement precision for alkali-metal atoms has reached the 10^{-9} level [15]. Normally, hyperfine splitting combined with Zeeman effect is described by the Breit-Rabi formula [16]. With the aforementioned measurement precision higher-order correction [17] of the Breit-Rabi formula may influence the experiment results, such as diamagnetic contributions to the interaction between the atom and the magnetic field [18]. Thus the comparison of the experiment results under conditions of low magnetic field and high magnetic field is necessary. In this paper we measure the ground-state hyperfine constant of $^{25}Mg^{+}$ under near zero magnetic-field condition by a rf resonant method in a linear Paul trap [19] to a precision of 7×10^{-9}.

Figure 1 shows the relevant energy levels of Mg atoms and $^{25}Mg^{+}$ ions. For a brief description of the measurement method, the ion is first initialized to the $|^2S_{1/2},F=2,m_F=0\rangle$ state. Then a microwave pulse that is resonant with the $|^2S_{1/2},F=2,m_F=0\rangle$ to $|^2S_{1/2},F=3,m_F=0\rangle$ transition (0-0 transition) is applied, and finally the $|^2S_{1/2},F=3,m_F=0\rangle$ state is detected through a resonant light with $|^2S_{1/2},F=3\rangle$ to $|^2P_{3/2},F=4\rangle$ at 280 nm.

Based on the 0-0 transition frequency measurements, we studied resonance frequency shifts and line broadening effect for the 0-0 transition. The main frequency shift comes from the ac magnetic field. It can be induced by the unbalanced rf currents in the linear Paul trap, and it can cause quadratic Zeeman shift in an ion optical clock, which is an important source for the ion clock systematic uncertainties [20,21]. Quadratic Zeeman shift caused by this field is evaluated by varying the rf drive power of the ion trap. Other shifts such as light shift and second-order Doppler shift are also discussed.

The experiment setup on the measurement of the hyperfine transition frequencies in the ground state of $^{25}Mg^{+}$ in a linear Paul trap is described in Sec. II. The experimental procedures are described in Sec. III. In Sec. IV, the experimental results are presented and discussed, followed with conclusions in Sec. V.

II. EXPERIMENTAL SETUP

A linear Paul trap is used to trap the magnesium ions. The linear Paul trap consists of four blade electrodes and two end-cap tip electrodes, as shown in Fig. 2. This structure allows better optical access for laser beams and fluorescence collection. The two opposing blade electrodes are fed with a high-voltage rf source and the other two are grounded. The distance between the two opposing blade electrodes is $2r=1.6$ mm. These four blade electrodes supply the radial confinement of trapped ions. The distance between the two end-cap tips is $2z=4.0$ mm. These two end-cap tip electrodes supply the axial confinement of trapped ions. Three copper rods are designed for compensation of stray electric fields in radial directions. Two of them are connected to form one electrode for horizontal compensation and the

*ke.deng@hust.edu.cn
†zehuanglu@hust.edu.cn

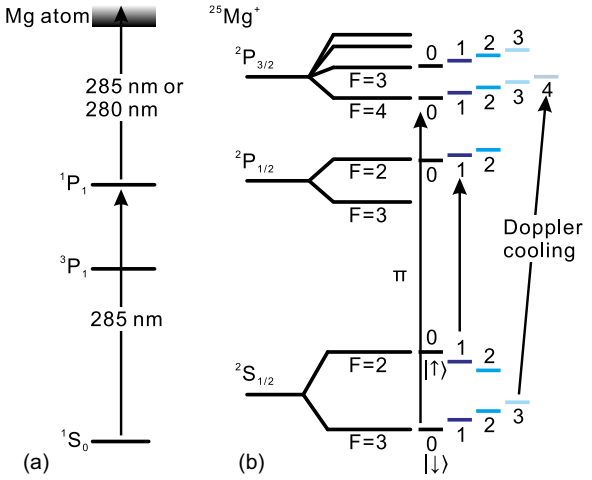

FIG. 1. (a) The relevant energy levels of the Mg atoms. (b) The relevant energy levels of $^{25}Mg^{+}$ ions. $|\downarrow\rangle$ denotes the $|^2S_{1/2}, F = 3, m_F = 0\rangle$ state and $|\uparrow\rangle$ denotes the $|^2S_{1/2}, F = 2, m_F = 0\rangle$ state. In the figure only $m_F \geqslant 0$ states are shown.

other is for vertical compensation. The axial compensation is implemented on the end-cap tip electrodes. All of the trap electrodes are held by precision machined ceramic to maintain their relative positions. The machinable ceramic is mounted on a titanium holder, which is installed on the bottom of the vacuum chamber [22].

A high-voltage rf power supply is needed to trap the ions. In our setup, this high rf voltage at a frequency of 23.76 MHz is first produced by a frequency synthesizer, and then amplified by an rf amplifier. Finally a homemade helical resonator [23] with quality factor of about 300 is used to supply the voltage on the blade electrodes. The input power into the resonator as well as the reflected power can be measured by an rf power meter, which is connected between the rf amplifier and the helical resonator.

Two fused silica reentrant viewports are installed on the vacuum chamber to collect the fluorescence signal of the ions. Two sets of imaging lens system are installed; one is for a photon counting module and the other is for an electron-multiplying CCD. The fluorescence collection efficiency is

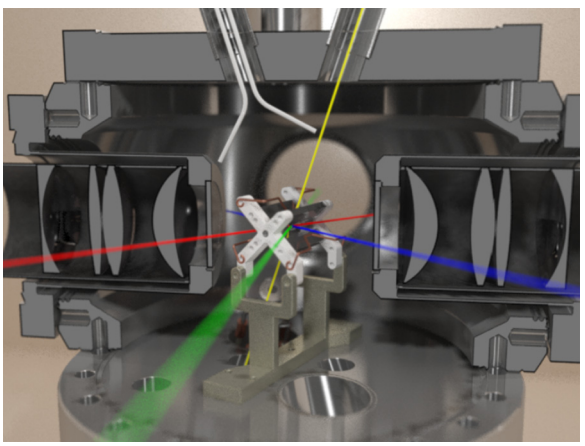

FIG. 2. Schematic of the experiment system.

0.4%. The pressure in the chamber is 10^{-8} Pa. Three pairs of Helmholtz coils are mounted around the vacuum chamber to compensate background magnetic field and to define the ion quantization axis. These coils are powered by a precise current source with a relative current drift less than 2×10^{-5} in 1 h.

A magnesium oven is installed on the bottom of the ion trap. Mg atoms are photoionized and then trapped and Doppler cooled. The ionization laser is a frequency-quadruple tunable diode laser system with wavelength at 285 nm. A Doppler cooling laser at 280 nm and repumping laser at 279 nm are also frequency-quadrupled diode laser systems. The output power is 2, 12, and 23 mW, respectively, and their linewidths are all measured to be less than 2 MHz.

A quarter-wave antenna made by copper with a designed resonant frequency of 1.79 GHz is installed outside the vacuum chamber. The top left of Fig. 2 shows the shape of the antenna. The angle of antenna is set to be 60 deg instead of 180 deg. During the experiment all the rf sources are referenced to a 5-MHz output of a cesium-beam clock with a specified accuracy of 5×10^{-13}.

III. EXPERIMENTAL PROCEDURES

During the magnesium oven operation, the 285-nm ionization laser and the 280-nm Doppler cooling laser intercept the atomic beam at the center of the ion trap. In the beginning, a 285-nm photon drives the Mg transition between $^1S_0 \rightarrow {}^1P_1$ states. Then the electron in the $^1P_1$ state reaches continuum by further absorbing another 285-nm photon. The frequency of the Doppler cooling laser is red-detuned 400 MHz with respect to the $^{25}Mg^{+}\ {}^2S_{1/2} \rightarrow {}^2P_{3/2}$ cycling transition [24,25].

In order to measure the ground-state hyperfine constant, a convenient method is to measure the hyperfine splitting frequency. For $^{25}Mg^{+}$ ions the nuclear spin is 5/2, so the ground-state hyperfine splitting shift can be expressed by the hyperfine constant:

$$\Delta E_{\mathrm{HFS}} = \tfrac{1}{2}hA[F(F+1) - I(I+1) - J(J+1)]. \quad (1)$$

Substituting $I = 5/2, J = 1/2$, and $F = 2,3$ into Eq. (1), the hyperfine splitting frequency ν_{HFS} of $^{25}Mg^{+}$ is proportional to the hyperfine structure constant, that is, $\nu_{\mathrm{HFS}} \equiv (E_{\mathrm{HFS}}|_{F=3} - E_{\mathrm{HFS}}|_{F=2})/h = 3A$. In practice, background magnetic field will always be present and will remove the degeneracy of Zeeman sublevels. To precisely measure the hyperfine splitting, the transition frequency of the 0-0 transition is measured. For convenience, we denote the states $|^2S_{1/2}, F = 3, m_F = 0\rangle$ and $|^2S_{1/2}, F = 2, m_F = 0\rangle$ to be $|\downarrow\rangle$ and $|\uparrow\rangle$ states respectively, as shown in Fig. 1. There is no linear Zeeman shift for the 0-0 transition, therefore quadratic Zeeman shift will dominate the 0-0 transition frequency shift. Thus the 0-0 transition frequency measurements in different magnetic fields are accomplished by measuring the Rabi spectra of the transition.

Since the applied magnetic-field strength depends linearly on the applied current on the Helmholtz coils, by fitting the measured curve with the applied current the hyperfine splitting in zero magnetic field can be deduced, and there is no need to measure the absolute magnetic-field strength. The frequency measurement always gives a positive value, so the sign of the hyperfine constant should be determined in another way.

By noticing the fact that the frequency of cycling transition $|^2S_{1/2}, F = 3, m_F = 3\rangle$ to $|^2P_{3/2}, F = 4, m_F = 4\rangle$ is 1.8 GHz higher than the frequency of transition $|^2S_{1/2}, F = 2, m_F = 2\rangle$ to $|^2P_{3/2}, F = 3, m_F = 3\rangle$, we can conclude that the state $|^2S_{1/2}, F = 3, m_F = 3\rangle$ should be the lower state. This means that the hyperfine structure constant of $^{25}Mg^{+}$ is negative.

The 0-0 transition Rabi spectra are recorded with the following sequence. At first, the magnesium ion is Doppler cooled for 1 ms with a 40-MHz red-detuned Doppler cooling laser. Then the ion is optically pumped to the $|\uparrow\rangle$ state by applying two π polarized lights simultaneously for 50 μs the frequencies of which are near the D_1 transition $|^2S_{1/2}, F = 2\rangle \rightarrow |^2P_{1/2}, F = 2\rangle$ and the D_2 transition $|^2S_{1/2}, F = 3\rangle \rightarrow |^2P_{3/2}, F = 2\rangle$, respectively. After this optical pumping the probability of the ion staying in the $|\uparrow\rangle$ state is about 65%. For the other cases the ion is randomly located on the other Zeeman sublevels of the $F = 2$ state. For these Zeeman sublevels there are linear Zeeman shifts. For example, the frequency of the transition $|^2S_{1/2}, F = 2, m_F = \pm 1\rangle \rightarrow |^2S_{1/2}, F = 3, m_F = 0\rangle$ is shifted from the 0-0 transition with a coefficient of $\mp 4.67 \times 10^9$ Hz/T. During our experiment the magnetic field can separate the $|^2S_{1/2}, F = 2, m_F = \pm 1\rangle \rightarrow |^2S_{1/2}, F = 3, m_F = 0\rangle$ transition and the 0-0 transition spectrum. Consequently, these unwanted initial states act as dark states during the experiment. It will lower the measured transition probability to about 65% compared with the pure $|\uparrow\rangle$ state. The relative frequency shift caused by line pulling effect is only 9×10^{-12} for a magnetic field of 1μT when all the unwanted initial states are in the nearest Zeeman sublevel. Then a microwave pulse that is resonant with the $|\uparrow\rangle \rightarrow |\downarrow\rangle$ transition is applied, followed by a 30-μs fluorescence detection pulse. The laser used in fluorescence detection is the same one as in the Doppler cooling. Typically, in 30 μs the $|\downarrow\rangle$ state, i.e. the bright state, will produce a mean photon number of 5.8, whereas for the $|\uparrow\rangle$ state, i.e. the dark state, only 0.2 photons can be collected. We use the threshold detection method for calculating the transition probability. For dark and bright states, the number of collected photons n obeys Poisson distribution with index of λ_D and λ_B, respectively. After rf interrogation the $^{25}Mg^{+}$ ion will stay in a superposition state $|\phi\rangle = c_1|\uparrow\rangle + c_2|\downarrow\rangle$. In order to obtain the transition probability c_2^2, the measurement is repeated for N times. We set a threshold n_0, and suppose that among the total N times there are x times that the number of collected photons is larger than n_0. It is straightforward to find out that x obeys the following distribution:

$$p(x) = \binom{N}{x}\lambda^x(1-\lambda)^{N-x}, \tag{2}$$

where $\lambda = c_1^2 P_1 + c_2^2 P_2$. $P_1(P_2)$ is defined as the probability that the number of collected photons is larger than n_0 when the ion is in the dark (bright) state. Considering the fact $c_1^2 + c_2^2 = 1$, the estimation of transition probability $\widehat{c_2^2}$ is

$$\widehat{c_2^2} = \frac{x/N - P_1}{P_2 - P_1}. \tag{3}$$

The variance of this estimation is

$$\mathrm{var}\left(\widehat{c_2^2}\right) = \frac{\hat{\lambda}(1-\hat{\lambda})}{N(P_2 - P_1)^2}. \tag{4}$$

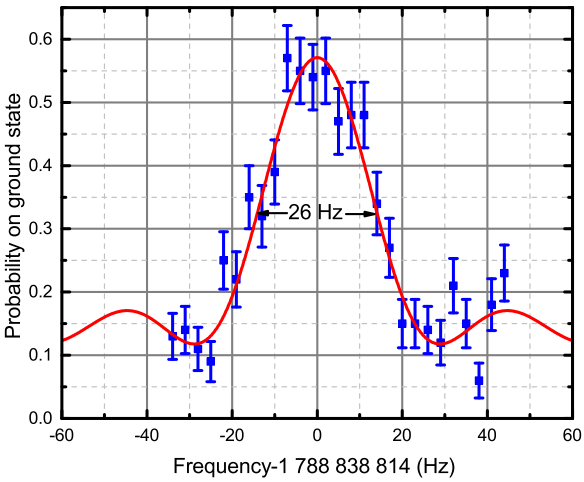

FIG. 3. Typical Rabi spectrum of the 0-0 transition. Each data point is averaged for 100 times.

Here $\hat{\lambda}$ is the estimation of λ. For $\lambda_D = 0.2$ and $\lambda_B = 5.8$, the $P_2 - P_1$ is maximized when $n_0 = 1$. Therefore we choose $n_0 = 1$ as the threshold. When $n_0 = 1$, $P_1 = 0.018$ and $P_2 = 0.979$. For a transition probability of 0.5, the variance of the estimation of transition probability is 0.0027, and the standard error is 0.052. The error caused by quantum projection noise is calculated through Eq. (4) and is shown in Fig. 3. These errors have already taken into account the population overlap between the bright state and the dark state.

The microwave frequency is scanned to record the Rabi spectrum. For every frequency point, the sequence described above is repeated for 100 times to calculate the transition probability.

Longer microwave π pulse time is always preferred in the experiment, because this means a narrower Fourier-transform linewidth for the spectrum. But decoherence between the two states of the 0-0 transition will limit the further increasing of the microwave interaction duration. The decoherence time can be estimated by measuring the probability of the ion decay to the $|\downarrow\rangle$ state over time which is initially pumped to the $|\uparrow\rangle$ state. Figure 3 shows the Rabi spectrum of the 0-0 transition with 30-ms microwave π pulse time. The signal-to-noise ratio is about 8. We find that the contrast of the Rabi spectrum decreases as we increase the interaction time. We use the contrast change in the Rabi spectrum to evaluate the decoherence time in our system, and the decoherence time is about 100 ms. The sources of decoherence are complicated. They could be due to the leakage of the pumping light during the coherent operation, the spectrum noise of the microwave source, the electromagnetic radiation from the trap rf fields, and fluctuations of the background magnetic field. The signal-to-noise ratio will be less than 1 if the interaction time is larger than 200 ms. To obtain the highest frequency accuracy we set the microwave π pulse time to be 30 ms.

To obtain the hyperfine splitting value, 0-0 transition frequency ν_{0-0} is measured three times at different bias magnetic fields. In order to eliminate error that is caused by possible linear drift of the current source, the current of every measurement is randomly picked in a preset value set. Since

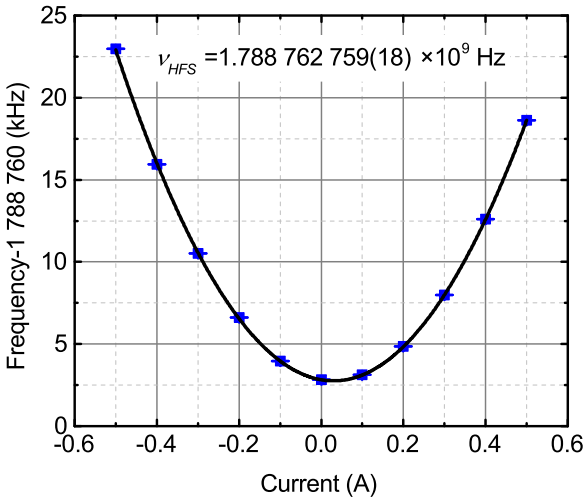

FIG. 4. Zeeman shift of $^{25}Mg^+$. Every point is an average of three measurements. The fitting model is given by Eq. (5). The hyperfine splitting frequency given by the fitting is $\nu_{\rm HFS} =$ 1.788 762 759(18) GHz. Another two independent parameters are $\frac{1}{2}(g_J - g_I)^2\mu_B^2\eta^2 = 2.567(50) \times 10^{14}$ Hz^2/A^2 and $I_0 = 2.98(3) \times 10^{-2}$ A, respectively.

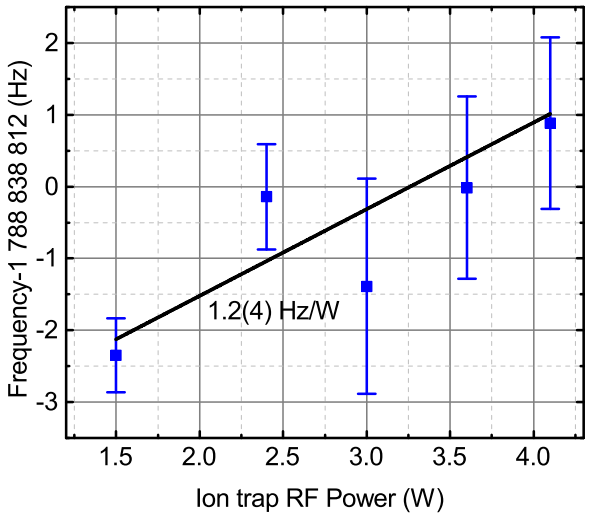

FIG. 5. The resonant frequency as a function of the rf drive power P. The experiment is done with 1-A bias current.

the bias magnetic field depends linearly on the applied current, the measured 0-0 transition frequency ν_{0-0} can be written as a function of the applied current I:

$$\nu_{0-0} = \sqrt{\nu_{\rm HFS}^2 + \tfrac{1}{2}(g_J - g_I)^2\mu_B^2\eta^2(I - I_0)^2}, \qquad (5)$$

where μ_B is the Boltzmann constant; I_0 is the bias current when magnetic field is zero; g_J and g_I are the electron total angular momentum g factor and nuclear angular momentum g factor, respectively; and η denotes the coefficient between the applied current and the magnetic-field strength. The data are then fit with the model described by Eq. (5) as shown in Fig. 4. Three independent parameters are given by the fittings, which are $\nu_{\rm HFS} = 1.788\ 762\ 759(18)$ GHz, $\frac{1}{2}(g_J - g_I)^2\mu_B^2\eta^2 = 2.567(50) \times 10^{14}$ Hz^2/A^2, and $I_0 = 2.98(3) \times 10^{-2}$ A, respectively.

IV. RESULTS AND DISCUSSION

Several effects will influence the accuracy of the measurement results. The main effect is caused by the quadratic Zeeman shift due to external magnetic-field perturbation. The quadratic Zeeman shift $\Delta\nu$ is proportional to the mean squares of the magnetic-field strength $\langle B^2\rangle$:

$$\Delta\nu = \frac{(g_J - g_I)^2\mu_B^2}{2h^2\nu_{\rm HFS}}\langle B^2\rangle. \qquad (6)$$

Zeeman effect will induce fluctuations in the measurement results and will also contribute to the frequency shifts. Magnetic-field fluctuations, from current supplies of Helmholtz coils, 50-Hz power line radiation, and environmental magnetic-field fluctuation, lead to nonideal repeatability of frequency measurements.

The presence of the uncompensated earth magnetic field perpendicular to the quantization axis will induce a small quadratic Zeeman shift during experiment. This residual magnetic field will make the measured hyperfine transition frequency a little higher. To minimize the earth magnetic field, $|^2S_{1/2}, F = 3, m_F = 3\rangle \rightarrow |^2S_{1/2}, F = 2, m_F = 2\rangle$ and $|^2S_{1/2}, F = 3, m_F = -3\rangle \rightarrow |^2S_{1/2}, F = 2, m_F = -2\rangle$ transition frequencies are measured under different bias magnetic fields. Since the linear Zeeman effect dominates the frequency shift, we linearly fit the data to find the cross point of the two curves which indicate the magnetic-field null point. This experiment is done in all three axes to ensure the earth magnetic field is canceled. The compensation accuracy is within 10 μT. This value will only induce a quadratic Zeeman shift as small as 4 mHz, which can be neglected. Here we consider a 100% uncertainty for this shift to be a conservative limit.

The stability of the output current of the current source for the Helmholtz coils is affected by the environmental temperature. By using smaller operating current, this effect can be decreased. The maximum shift is present at the point of maximum magnetic-field strength. Typically the maximum frequency shift caused by environment temperature change is 5 Hz with 0.5-A applied current. Moreover, some unknown magnetic-field source appears randomly. This will make a large frequency jump as large as 30 Hz at 0.5-A applied current in day to day operation. We include all the data in the final results. They contributed to the statistical error bar of the final results.

In principle the 50-Hz power line radiation can be eliminated by triggering every measurement with the power line signal. The measured background magnetic-field fluctuation with a fluxgate magnetometer is 1 μT peak to peak. This contributes a 0.2-Hz shift to transition frequency. So we do not trigger our measurement in order for faster data taking. Here we consider a 100% uncertainty for this shift to be a conservative limit.

Due to charge dissipation and patch potential variation during experiment or after each ion loading, the position of the ions will drift. Hence the magnetic-field strength felt by the ions may vary. To evaluate the field change in different positions, we measure the magnetic sensitive $|^2S_{1/2}, F = 3, m_F = 3\rangle \rightarrow |^2S_{1/2}, F = 2, m_F = 2\rangle$ transition frequency in different positions. The result shows that the magnetic-field

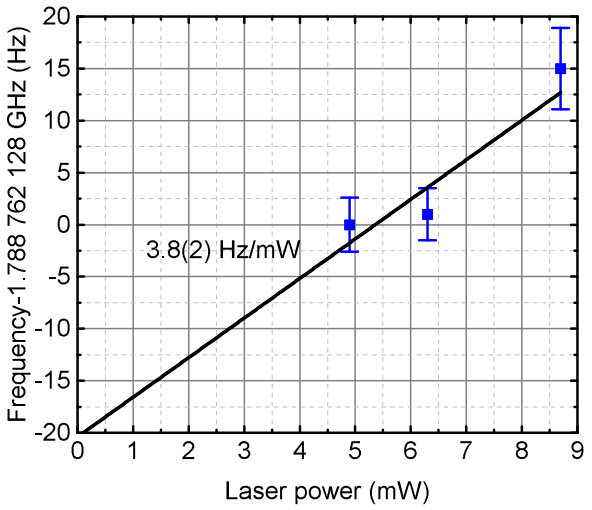

FIG. 6. The resonant frequency as a function of the incident laser power.

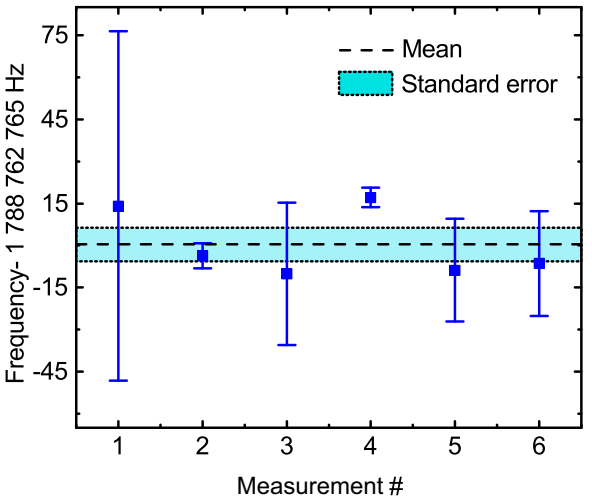

FIG. 7. Summary of the measurements of the $^{25}Mg^{+}$ hyperfine splitting. Six experiment runs are used to determine the final frequency. All error bars are drawn according to fitting standard error. The mean value is calculated to be 1.788 762 765(12) GHz.

strength change is less than 10 nT in 10-μm distance, which means even with 0.3-mT magnetic field the frequency shift caused by this effect will not exceed 1 Hz. Thus ion position change does not have a significant effect on the final results in this paper.

An ac magnetic field caused by the unbalanced rf current will be present during experiment. Quadratic Zeeman shift caused by this field is evaluated by varying the rf drive power of the ion trap. Since the unbalanced rf current depends linearly on the square root of the rf power, the frequency shift will be proportional to the rf power. As shown in Fig. 5 the 0-0 transition frequency depends weakly on rf power. This indicates that the ac magnetic-field amplitude is about 2 μT. During measurement rf power is fixed at 3.0 W, thus the rf power induced shift is 3.6 Hz. Here we consider a 100% uncertainty for this shift to be a conservative limit.

Light shift shall also be taken into account due to the leakage of the Acousto-optic modulator (AOM) switches. We use different laser powers to measure the 0-0 transition frequency. The maximum power is two times higher than the minimum power. The results show a frequency shift of 3.8(2) Hz/mW, as shown in Fig. 6. During experiment we fix the laser power to be 5 mW, which means the light shift would be 19(1) Hz.

A single magnesium ion is laser cooled to near its Doppler limit with a typical average vibration quantum number of 17. The heating rate of the ion trap is measured to be 22 phonons per second. That means the vibration quantum number will be below 20 during the experiment. Even taking $\bar{n} = 20$ as the upper limit, the second-order Doppler shift due to secular motion is a few tens of microhertz, which can be neglected. The calculated second-order Doppler shift due to micromotion is far less than microhertz, so it also can be neglected.

The ground-state hyperfine splitting for the $^{25}Mg^{+}$ ion is measured to be 1.788 762 765(12) GHz, as shown in Fig. 7. The hyperfine constant A calculated due to Eq. (1) is -596.254 255(4) MHz. Since except for light shift the total frequency shift discussed above is much smaller than the statistical error of the experiment, all these shifts are taken as systematic uncertainty (see Table I). Taking the total shift into account the final result gives the hyperfine constant for the $^{25}Mg^{+}$ ion as -596.254 248 7(42) MHz. This result has one order of magnitude better accuracy than that of the previous result [4]. There is a 120-Hz difference between these two results which is not within the stated error bar. One consideration is this difference may rise from diamagnetic shifts. Currently, there is no reported theoretical calculation of the diamagnetic shift of the $^{25}Mg^{+}$ ion. If the relative diamagnetic shift is comparable with ^{85}Rb ($5.8 \times 10^{-10}/T^2$) and $^{9}Be^{+}$ ($2.63 \times 10^{-11}/T^2$), the diamagnetic shift at 1.24 T will be no more than 0.6 Hz. Another possible reason is the higher-order correction of the Breit-Rabi formula. Using the modified Breit-Rabi formula [17] and the data given by [4] to recalculate the hyperfine constant A shows that there is no difference in comparison with the results using the original Breit-Rabi formula. Since the hyperfine constant

TABLE I. Errors budget of the measured hyperfine structure constant.

Term	Shifts (Hz)	Uncertainty (Hz)	Limitation
dc quadratic Zeeman	0	0.001	Uncompensated earth magnetic field
ac quadratic Zeeman	0	0.07	Background ac magnetic field (<3 MHz)
ac quadratic Zeeman	0	1.2	Trap rf magnetic field (23.76 MHz)
Light shift	6.3	0.4	AOM leakage
Statistical		4	
Total	6.3	4.2	

appears as a common factor in all equations, it makes the hyperfine constant insensitive to the correction formula.

V. CONCLUSION

In conclusion, we measured the ground-state hyperfine constant of the $^{25}Mg^{+}$ ion in a linear Paul trap under low magnetic field. The measurement is performed with a single ion, and offers valuable comparison with a previous result [4]; it is performed in a Penning trap under large magnetic field and with multiple ions. The measured ground-state hyperfine constant for the $^{25}Mg^{+}$ ion is $-596.254\,248\,7(42)$ MHz, which has one order of magnitude better precision than the previous result [4]. There is a 127-Hz difference between the two results that cannot be accounted for at the moment, suggesting more theoretical and experimental works need to be performed to find out the reasons.

ACKNOWLEDGMENTS

The project is partially supported by the National Basic Research Program of China (Grant No. 2012CB821300) and the National Natural Science Foundation of China (Grants No. 11304109, No. 11174095, and No. 91336213).

[1] V. Gerginov, N. Nemitz, S. Weyers, R. Schröder, D. Griebsch, and R. Wynands, Metrologia **47**, 65 (2009).
[2] Y. Ovchinnikov and G. Marra, Metrologia **48**, 87 (2011).
[3] K. Okada, M. Wada, T. Nakamura, A. Takamine, V. Lioubimov, P. Schury, Y. Ishida, T. Sonoda, M. Ogawa, Y. Yamazaki, Y. Kanai, T. M. Kojima, A. Yoshida, T. Kubo, I. Katayama, S. Ohtani, H. Wollnik, and H. A. Schuessler, Phys. Rev. Lett. **101**, 212502 (2008).
[4] W. M. Itano and D. J. Wineland, Phys. Rev. A **24**, 1364 (1981).
[5] R. Blatt and G. Werth, Phys. Rev. A **25**, 1476 (1982).
[6] H. Knab, K. Niebling, and G. Werth, IEEE Trans. Instrum. Meas. **34**, 242 (1985).
[7] J. W. Zhang, Z. B. Wang, S. G. Wang, K. Miao, B. Wang, and L. J. Wang, Phys. Rev. A **86**, 022523 (2012).
[8] F. G. Major and G. Werth, Phys. Rev. Lett. **30**, 1155 (1973).
[9] R. Blatt, H. Schnatz, and G. Werth, Phys. Rev. Lett. **48**, 1601 (1982).
[10] C. Sur, B. K. Sahoo, R. K. Chaudhuri, B. P. Das, and D. Mukherjee, Eur. Phys. J. D **32**, 25 (2005).
[11] S. Ahmad, J. Andriessen, and T. P. Das, Phys. Rev. A **27**, 2790 (1983).
[12] M. S. Safronova, A. Derevianko, and W. R. Johnson, Phys. Rev. A **58**, 1016 (1998).
[13] B. K. Mani and D. Angom, Phys. Rev. A **81**, 042514 (2010).
[14] J.-L. Heully and A.-M. Mårtensson-Pendrill, Phys. Scr. **31**, 169 (1985).
[15] A. Beckmann, K. D. Böklen, and D. Elke, Z. Phys. **270**, 173 (1974).
[16] G. Breit and I. I. Rabi, Phys. Rev. **38**, 2082 (1931).
[17] D. L. Moskovkin and V. M. Shabaev, Phys. Rev. A **73**, 052506 (2006).
[18] N. Shiga, W. M. Itano, and J. J. Bollinger, Phys. Rev. A **84**, 012510 (2011).
[19] W. Paul, Rev. Mod. Phys. **62**, 531 (1990).
[20] W. H. Oskay, S. A. Diddams, E. A. Donley, T. M. Fortier, T. P. Heavner, L. Hollberg, W. M. Itano, S. R. Jefferts, M. J. Delaney, K. Kim, F. Levi, T. E. Parker, and J. C. Bergquist, Phys. Rev. Lett. **97**, 020801 (2006).
[21] T. Rosenband, D. B. Hume, P. O. Schmidt, C. W. Chou, A. Brusch, L. Lorini, W. H. Oskay, R. E. Drullinger, T. M. Fortier, J. E. Stalnaker, S. A. Diddams, W. C. Swann, N. R. Newbury, W. M. Itano, D. J. Wineland, and J. C. Bergquist, Science **319**, 1808 (2008).
[22] H. Che, K. Deng, Z. T. Xu, W. H. Yuan, J. Zhang, and Z. H. Lu, Phys. Rev. A **96**, 013417 (2017).
[23] K. Deng, Y. L. Sun, W. H. Yuan, Z. T. Xu, J. Zhang, Z. H. Lu, and J. Luo, Rev. Sci. Instrum. **85**, 104706 (2014).
[24] G. Clos, M. Enderlein, U. Warring, T. Schaetz, and D. Leibfried, Phys. Rev. Lett. **112**, 113003 (2014).
[25] V. Batteiger, S. Knünz, M. Herrmann, G. Saathoff, H. A. Schüssler, B. Bernhardt, T. Wilken, R. Holzwarth, T. W. Hansch, and T. Udem, Phys. Rev. A **80**, 022503 (2009).